Impairment of sugar transport in the vascular system acts on nitrogen remobilization and nitrogen use efficiency in Arabidopsis

Beate Hoffmann, Emilie Aubry, Anne Marmagne, Sylvie Dinant, Fabien Chardon, Rozenn Le Hir

Received: 26 September 2022 | Revised: 11 November 2022 | Accepted: 16 November 2022

DOI: 10.1111/ppl.13830

ORIGINAL RESEARCH

Physiologia Plantarum

Impairment of sugar transport in the vascular system acts on nitrogen remobilization and nitrogen use efficiency in Arabidopsis

Beate Hoffmann | Emilie Aubry | Anne Marmagne | Sylvie Dinant | Fabien Chardon | Rozenn Le Hir

Université Paris-Saclay, INRAE, AgroParisTech, Institut Jean-Pierre Bourgin (IJPB), Versailles, France

Correspondence
Rozenn Le Hir, Université Paris-Saclay, INRAE, AgroParisTech, Institut Jean-Pierre Bourgin (IJPB), 78000, Versailles, France.
Email: rozenn.le-hir@inrae.fr

Funding information
Saclay Plant Sciences, Grant/Award Number: ANR-17-EUR-0007

Edited by C.H. Foyer

Abstract

Carbon (C) and nitrogen (N) metabolisms have long been known to be coupled, and this is required for adjusting nitrogen use efficiency (NUE). Despite this intricate relationship, it is still unclear how deregulation of sugar transport impacts N allocation. Here, we investigated in Arabidopsis the consequences of the simultaneous downregulation of the genes coding for the sugar transporters SWEET11, SWEET12, SWEET16, and SWEET17 on various anatomical and physiological traits ranging from the stem's vascular system development to plant biomass production, seed yield, and N remobilization and use efficiency. Our results show that intracellular sugar exchanges mediated by SWEET16 and SWEET17 proteins specifically impact vascular development but do not play a significant role in the distribution of N. Most importantly, we showed that the double mutant *swt11 swt12*, which has an impacted vascular development, displays an improved NUE and nitrogen remobilization to the seeds. In addition, a significant negative correlation between sugar and amino acids contents and the inflorescence stem radial growth exists, highlighting the complex interaction between the maintenance of C/N homeostasis and the inflorescence stem development. Our results thus deepen the link between sugar transport, C/N allocation, and vascular system development.

1 | INTRODUCTION

Carbon (C) and nitrogen (N) are essential and limiting elements for plant, animal, and microorganism growth. In plants, the tricarboxylic acid cycle is the primary source of C skeletons required for ammonium assimilation and is linked to the amino acid metabolism by the glutamate dehydrogenase, thus bridging C and N metabolisms (Hodges, 2002; Huppe & Turpin, 1994). In addition, N plays a significant role in C metabolism due to its function in Rubisco synthesis. At the same time, C compounds are essential for N absorption, nitrate reduction, N_2 fixation, and amino acid metabolism to generate C skeletons, metabolic energy, and reductants (Baslam et al., 2021). To successfully reproduce, plants must constantly adjust their C and N contents. Such modulation can be achieved at various levels, ranging from the modulation of nutrient assimilation proteins' activity and the control of nutrient transport to a variety of mechanisms controlling the expression of genes encoding the proteins involved in nutrient metabolism, transport, and signaling. This has been exemplified in many studies which focused on improving C/N metabolism and transport to reach higher plant yield (Braun et al., 2014; Marmagne et al., 2022; The et al., 2021).

To reach the seeds, sugars, and amino acids, which are the primary products of C and N metabolisms, are transported through the vasculature (i.e., xylem and phloem) (van Bel, 2021). It is now well established that the main C pools are delivered long distance from the phloem, whereas the N pools are provided from both xylem and phloem. A third significant transport pathway is the lateral transfer of sugars and amino acids between phloem and xylem and vice versa

(Aubry et al., 2019; Tegeder & Masclaux-Daubresse, 2018). To ensure an appropriate distribution of sugars and amino acids at the whole plant level, nutrients can move through the plasmodesmata (symplasmic pathway), even if experimental proof of such a transport pathway for amino acids is still lacking (Kim et al., 2021a), or by specialized transporters such as sugar will eventually be exported transporters (sweet), usually multiple acids move in and out transporters (UmamiTs), sucrose transporters (SUC), and the amino acid permeases (AAPs) (Ladwig et al., 2012; Müller et al., 2015; Tegeder & Masclaux-Daubresse, 2018; Xue et al., 2022). Overall, the delivery of nutrients from cell to cell and at long distance encompasses an intricate network between the metabolism products and their transport pathways that *in fine* creates sources (e.g., leaves and stems) and sink organs (e.g., seeds, roots). These specialized transporters proteins are expressed in different plant organs (roots, leaves, stem, seeds), tissues (xylem, phloem, parenchyma cells, mesophyll cells), and subcellular compartment (plasma membrane or tonoplast), suggesting that tight coordination of their transport activities is needed for every step of plant development and growth. In this respect, genetic modifications have been used to understand the contributory role of sugar and amino acid transporter genes in increasing the C and N nutrition of seeds in crop and non-crop species (Grant et al., 2021; Lu et al., 2020; Wingenter et al., 2010; Zhang et al., 2010). For instance, the concurrent overexpression of AAP1 and SUT1 in pea increased the nutrient fluxes from source to sink, resulting in increased seed number and protein content (Grant et al., 2021). Nonetheless, despite the need to develop new strategies to improve plant yield and quality, experimental data regarding the impact of deregulation of sugar transport on N allocation or amino acids transport on C allocation is still scarce (Lu et al., 2020; Perchlik & Tegeder, 2018).

In this work, we proposed to fill this gap by evaluating the consequences of deregulating members of the SWEET sugar transporter family on biomass production, seed yield, and N allocation in Arabidopsis. Especially SWEET11 and SWEET12 have been shown to be involved in the transport of sucrose and hexoses from vascular parenchyma cells in leaves and stems (Chen et al., 2012; Kim et al., 2021b; Le Hir et al., 2015). Interestingly, the regulation of their expression is part of the plant carbon and nitrogen acquisition coordination mediated by the transcription factor HY5 (Chen et al., 2016). In addition, the expression of *SWEET16* and *SWEET17*, which are coding for tonoplastic sugar transporters expressed in leaves, roots, and stems, are modified in response to N deficiency (Chardon et al., 2013; Klemens et al., 2013). Therefore, based on these previous works, we focused on the concurrent downregulation of *SWEET11*, *SWEET12*, *SWEET16*, and *SWEET17* genes. Moreover, those genes are also expressed in the inflorescence stem (Aubry et al., 2022; Le Hir et al., 2015), which is an obligatory route for the transport of nutrients from leaves to seeds; therefore, the inflorescence stem is of interest when studying whole plant C and N allocation. Overall, the analysis of the *swt11 swt12*, *swt16 swt17* double mutants, and the *swt11 swt12 swt16 swt17* quadruple mutant allowed us to establish a link between the sugar transport between the different vascular cell types, nitrogen use efficiency (NUE) and nitrogen remobilization efficiency (NRE) in the seeds.

2 | MATERIALS AND METHODS

2.1 | Plant material and growth conditions

To obtain the quadruple mutant *sweet11-1sweet12-1sweet16-4sweet17* (hereafter referred to as *swt-q*), we crossed the *sweet11-1-sweet12-1* (hereafter referred to as *swt11 swt12*) double mutant (Le Hir et al., 2015) with the *sweet16-4sweet17-1* (hereafter referred as *swt16 swt17*) double mutant (Aubry et al., 2022). Homozygous plants were genotyped using gene-specific primers in combination with a specific primer for the left border of the T-DNA insertion (Table S1). By using RT-PCR (reverse transcriptase polymerase chain reaction) analysis, we confirmed that full-length transcripts of *SWEET11*, *SWEET12*, *SWEET16*, and *SWEET17* cannot be amplified in the *swt-q* mutant line (Figure S1 and Table S1 for primers sequences). To synchronize germination, seeds were stratified at 4°C for 48 h and sown in the soil in a growth chamber in long-day conditions (16 hday/8 h night and 150 µE m^{-2} s^{-1}) at 22/18°C (day/night temperature) with 35% relative humidity. Plants were watered with Plant-Prod nutrient solution twice a week (Fertil).

2.2 | GUS staining

The lines expressing pSWEET11:SWEET11-GUS or pSWEET12:SWEET12-GUS (Chen et al., 2012) and pSWEET16:SWEET16-GUS or pSWEET17:SWEET17-GUS (Guo et al., 2014) in Col-0 background were used to assess SWEET11, SWEET12, SWEET16, and SWEET17 expression pattern on seven-week-old plants grown in the greenhouse. The histochemical GUS (Beta-glucuronidase) staining was performed according to Sorin et al. (2005). Inflorescence stems subjected to GUS staining were then embedded in 8% (w/v) agarose and sectioned with a Leica VT100S vibratome. Sections were counterstained for lignin by phloroglucinol staining (Pradhan Mitra & Loqué, 2014). Pictures were taken using a Leitz Diaplan microscope equipped with an AxioCam MRc camera and the ZEN (blue edition) software package (Zeiss, https://www.zeiss.com/).

2.3 | Inflorescence stem growth and sample preparation

The main inflorescence stem height was measured with a ruler at 45 days after sowing (DAS) and the stem diameter was measured either on Image J with the Feret diameter tool (see next paragraph) or with a digital caliper at the bottom of the stem. At 45 DAS, a 1- to 2-cm segment was taken at the bottom part of the stem. Stem segments were embedded in an 8% agarose solution and sectioned with a VT100 S vibratome (Leica). Cross-sections were stained with a FASGA staining solution prepared as

described in Tolivia and Tolivia (1987) for morphometric analysis of the different stem tissues.

2.4 | Morphometric analysis of the stem tissues

Stained inflorescence stem cross-sections were imaged under an Axio Zoom V16 microscope equipped with a Plan-Neofluar Z 2.3/0.57 FWD 10.6 objective (Zeiss). For each section, several parameters were measured: stem diameter, stem area, vascular system area (combining the area of all the vascular bundles [VBs]), pith area, the phloem area (combining the phloem area of all VBs), the xylem area (combining the xylem area of all VBs) and the interfascicular thickness. The area of the other tissues (including epidermis, cortex, and interfascicular fibers) was then calculated by subtracting the sum of the pith, phloem, and xylem areas from the stem area. All parameters were measured using the Image J software package (Schneider et al., 2012). For the same sections, all the VBs were photographed individually using a confocal laser scanning microscope and the morphological analysis of the xylem was performed as described in Le Hir et al. (2015). For each VB, the morphological segmentation allowed access to the number of xylem cells (xylary fibers and xylem vessels) as well as their cross-sectional areas. Cells with a cross-sectional area comprised between 5 and 150 μm^2 were considered to be xylary fibers, and cells with a cross-sectional area greater than 150 μm^2 were considered to be xylem vessels. The sum of all xylem cell cross-sectional areas was then calculated to give the total xylem cross-sectional area. The average xylary fiber and xylem vessel area were calculated by dividing the total xylem cross-sectional area by the number of each cell type.

2.5 | Quantification of soluble sugars, starch, and total amino acids

The main inflorescence stems of wild type (WT), *swt11swt12*, *swt16swt17*, and *swt-q* mutants, without lateral stems, siliques and flowers, were harvested in the middle of the day (8 h after the beginning of the light period), frozen in liquid nitrogen and ground with a mortar and a pestle. Soluble sugars and starch were extracted from 50 mg of powder from an individual stem and quantified by the enzymatic method as described in Sellami et al. (2019). Briefly, the soluble sugars were extracted by two successive additions of 500 µl of 80% ethanol for 2 h in an ice bath. The supernatants were then separated from the residual solid material (containing starch), evaporated with a speed-vac, and re-suspended with water. For the starch quantification, the residual solid material obtained previously was hydrolyzed by amylo-glucosidase and α-amylase prior to glucose quantification. The sucrose, glucose, and fructose levels were then determined using an enzymatic sucrose/D-glucose/D-fructose kit (R-Biopharm). Total amino acids quantification was performed according to the protocol of Rosen (1957) and using glutamine as a standard. Nine biological replicates coming from two independent experiments were analyzed.

2.6 | Nitrogen and carbon percentage measurement and ^{15}N labeling experiment

The different genotypes were grown in a growth chamber as described above. Around 30 DAS, while plants are still at the vegetative stage, 1 ml of a 10 mM nitrate solution containing 10% of $^{15}NO_3$ was applied to the soil close to the plants' collar. Then, plants were left to grow until the end of their cycle and harvested once all seeds were matured and the rosette dried. Plants were separated into different samples: (1) rosette, (2) stem (including the main and lateral stems, cauline leaves, and empty dry siliques), and (3) seeds (total seeds). As plants were grown in soil, we could not harvest the roots without losing a large part of them. The dry weight (DW) of the different samples was determined. Then samples were ground to a homogenous fine powder and a subsample of 1000–2000 µg was precisely weighted in tin capsules to determine the C and N percentages (C% and N%) and the ^{15}N abundance using an elemental analyzer (FLASH 2000 Organic Elemental Analyzer, Thermo Fisher Scientific) coupled to an isotope ratio mass spectrometer (delta V isotope ratio mass spectrometer, Thermo Fisher Scientific) calibrated using international reference (caffeine, IAEA-600). The ^{15}N abundance along with the following parameters: harvest index (HI), N allocation in rosette, N allocation in stem, N allocation in seeds (nitrogen harvest index [NHI]), NUE (NUE = NHI/HI), ^{15}N allocation in rosette, ^{15}N allocation in stem, ^{15}N allocation in seeds (^{15}NHI) and NRE were calculated as described previously (Jasinski et al., 2021). The NRE index is calculated as the ratio between the ^{15}NHI (percentage of ^{15}N in seeds) over the plant HI (NRE = ^{15}NHI/HI). Finally, the proportion of N coming from remobilization or post-flowering uptake was calculated as described in Marmagne et al. (2022). The absolute quantity of C contained in each sample was defined as QtyC = DW × C%. The following formulas were then used to evaluate the parameters related to the C fluxes:

$$\text{C allocation in rosette} = \text{QtyC}_{\text{rosette}}/(\text{QtyC}_{\text{rosette}} + \text{QtyC}_{\text{stem}} + \text{QtyC}_{\text{seeds}}),$$

$$\text{C allocation in stem} = \text{QtyC}_{\text{stem}}/(\text{QtyC}_{\text{rosette}} + \text{QtyC}_{\text{stem}} + \text{QtyC}_{\text{seeds}}),$$

$$\text{C allocation in seeds} = \text{QtyC}_{\text{seeds}}/(\text{QtyC}_{\text{rosette}} + \text{QtyC}_{\text{stem}} + \text{QtyC}_{\text{seeds}}).$$

2.7 | RNA isolation, cDNA synthesis, and RT-PCR

RNAs were prepared from the main inflorescence stem from 7-week-old plants grown as described above. Samples were frozen in liquid nitrogen before being ground with a mortar and a pestle. Powders were stored at −80°C until use. Total ribonucleic acid (RNA) was extracted from frozen tissue using TRIzol® reagent (Thermo Fisher Scientific, 15595-026) and treated with DNase I, RNase-free (Thermo Fisher Scientific, EN0521). cDNA was synthetized by reverse transcribing 1 µg of total RNA using RevertAid H minus reverse transcriptase (Thermo Fisher Scientific, EP0452) with 1 µl of oligo(dT)18 primer (100 pmoles) according to the manufacturer's instructions. The reaction was stopped by incubation at 70°C for 10 min. Full-length

PCR was performed by using primers spanning the complete CDS for each gene tested (Table S1).

2.8 | Statistical analysis

One-way ANOVA combined with a Tukey's comparison post-test was done using R (version 4.0.2) and Rstudio (version 1.4.1103) software. A p-value < 0.05 was considered significant. Spearman correlations were realized using R with adjusted p-values calculated with Holm's method. Principal component analysis (PCA) was performed using the "FactoMineR" package of R (Le et al., 2008). The least-square means were calculated using the R package "emmeans".

3 | RESULTS

It is now established that modifications of the facilitated transport of sugar at the plasma membrane or the tonoplast lead to defects in the Arabidopsis shoot and root development (for review, see Xue et al., 2022). However, to what extent perturbations of sugar exchanges at both the plasma membrane and the tonoplast lead to defects in plant growth and development still needs to be explored. To address this question, we produced and characterized the *swt11 swt12 swt16 swt17* quadruple mutant (*swt-q*) along the corresponding *swt11 swt12*, and *swt16 swt17* double mutant lines (Aubry et al., 2022; Le Hir et al., 2015).

3.1 | The inflorescence stem growth and development are affected in the quadruple sweet mutant line

Alike *swt11 swt12*, the inflorescence stem of *swt-q* was shorter and thinner (by about 30%) than wild-type stem (Figure 1A–C). Moreover, as previously described, the stem of the *swt16 swt17* was thinner but not shorter than that of the wild type (Figure 1A–C) (Aubry et al., 2022). The stem height-to-diameter ratio of both double mutants and the *swt-q* mutant was similar to that of the wild-type plants (Figure 1D).

We further characterized the inflorescence stem growth and measured, 45 DAS, the portions of the stem corresponding to the cauline leaf zone, and to the "true inflorescence" (Pouteau & Albertini, 2009), the number of siliques, the density of siliques, and the number of lateral inflorescences (Figure 1E–H). In wild-type plants, the zone carrying the cauline leaves and the lateral inflorescence stems represents about 35% of the total inflorescence stem height, while about 65% is occupied by the true inflorescence zone (Figure 1E). Interestingly, we observed that the proportion of this latter is reduced in the *swt11 swt12*, and *swt-q* mutants compared to wild-type plants (Figure 1E). This phenotype is accompanied by a reduced number of siliques in the same genotypes (Figure 1F). Nonetheless, the silique density was not significantly different between all genotypes studied (Figure 1G). Finally, we did not observe any differences in the number of lateral inflorescences stems in any mutant lines compared to wild-type plants (Figure 1H). We also explored the tissue distribution within the stem cross-section by measuring the area occupied by the pith, phloem, xylem, and outer tissues (i.e., epidermis, cortex, and interfascicular fibers) as well as the thickness of the interfascicular fibers (Figure 1I,J). In our growth conditions, the pith represents about 47% of the wild-type stem cross-sectional area, while 14% is occupied by the vascular system (phloem and xylem). Finally, 39% of the total stem area is occupied by the epidermis, cortex, and interfascicular fibers. The results are in accordance with those previously published by Paul-Victor and Rowe (2011). Interestingly, the tissue organization changed in the different mutant lines (Figure 1I). Indeed, a significant decrease in the proportion of xylem tissue was measured in the *swt-q* mutant compared to the wild type, while no change in the proportion of phloem tissue was measured in any of the lines (Figure 1I), suggesting that the decrease in phloem area observed previously (Aubry et al., 2022; Le Hir et al., 2015) is proportional to the overall decrease of the stem cross-sectional area. Moreover, a decreased proportion of pith tissue along with an increased proportion of the outer tissue layers was measured in the *swt11 swt12*, and *swt-q* mutants. Additionally, the thickness of the interfascicular fibers was significantly smaller in all the mutant lines compared to the wild type (Figure 1J). Therefore, the stem radial growth phenotype could be associated with a defect in the stem tissue distribution with less xylem, pith, and interfascicular fibers.

Altogether these results show that both *swt11 swt12* and quadruple mutants display a similar phenotype, suggesting that adding perturbations of the cytosol-vacuole sugar exchanges (via disruption of the *SWEET16* and *SWEET17* expression) does not further affect the main inflorescence stem growth and development.

3.2 | Interplay between stem growth parameters and nutrient content

Both *swt11 swt12* and *swt16 swt17* double mutants have been shown to accumulate sugars in rosette leaves and inflorescence stems (Aubry et al., 2022; Chen et al., 2012; Gebauer et al., 2017). Moreover, it has been demonstrated that the content of metabolites such as sucrose, glutamine and starch is negatively correlated with rosette biomass production (Meyer et al., 2007; Sulpice et al., 2009). Here, we tested the correlation between stem growth parameters and stem nutrient content in the different genotypes by measuring the main inflorescence stem diameter and height along with the total soluble sugars (sucrose, glucose, and fructose), starch, and total amino acids content on the same samples (Figures 1 and 2). A significant increase of soluble sugars, starch, and amino acid contents was measured in the *swt11 swt12*, and *swt-q* mutant lines compared to the wild type (Figure 2). Additionally, we show that *swt16 swt17* stems also tend to accumulate soluble sugars compared to wild-type stems but not as much as the *swt11 swt12*, and *swt-q* mutant lines (Figure 2). We then computed correlation coefficients between these parameters

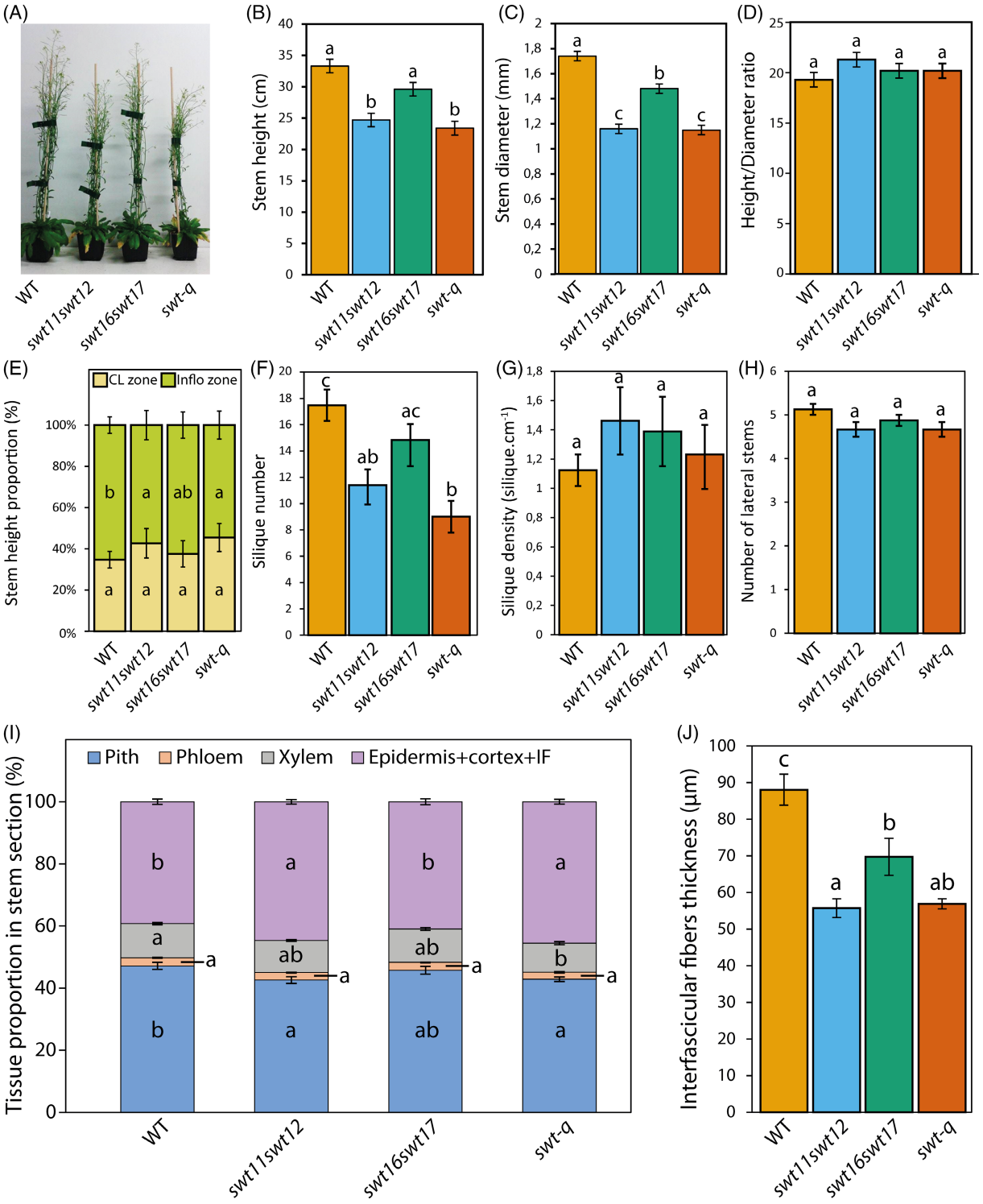

FIGURE 1 Main inflorescence growth and development are altered in the quadruple *sweet* mutant line. (A) Photographs of a representative plant of wild type, *swt11 swt12*, *swt16 swt17*, and quadruple mutants taken at 45 DAS. (B–D) Barplots showing the main inflorescence stem height (B), diameter (C), and the stem height-to-stem diameter ratio (D). Least-square means from three independent cultures ± SE ($n = 17$ for each genotype). Letters indicate statistical differences between genotypes according to an ANOVA and Tukey's comparison post-test. (E) Proportion of the stem occupied by the "cauline leaf zone" (CL zone) and the "true inflorescence zone" (Inflo zone). (F–H) Barplots showing the silique number (F), the silique density (G), and the number of lateral inflorescence stems (H). (I) Stacked barplot showing the distribution of tissues (epidermis+cortex+interfascicular fibers (IF), pith, phloem, and xylem) within an inflorescence stem cross-section; and (J) barplot showing the interfascicular fibers thickness among the different genotypes. Means ± SE ($n \geq 8$ plants for each genotype). Letters indicate statistical differences between genotypes according to an ANOVA and Tukey's comparison post-test.

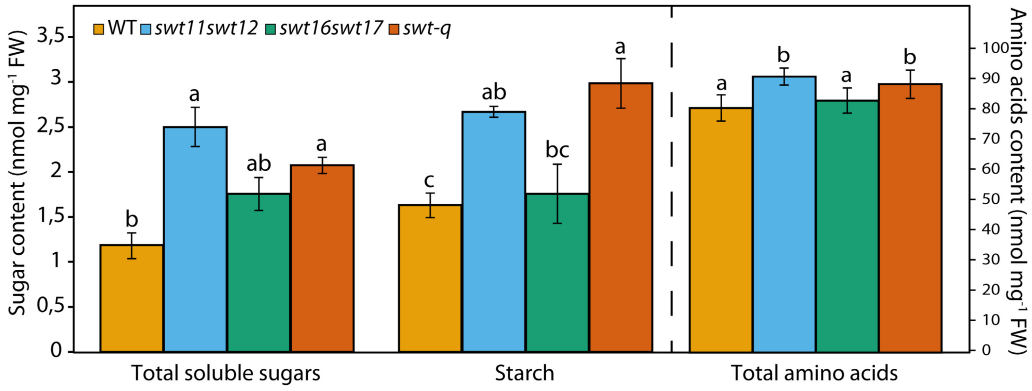

FIGURE 2 Soluble sugars, starch, and amino acids accumulate in the main inflorescence stem of multiple *sweet* mutants. Barplots the total soluble sugars, starch, and total amino acids content of wild type, *swt11 swt12*, *swt16 swt17*, and quadruple mutants. Least-square means from two independent experiments ± SE are shown ($n = 9$ for each genotype). Different letters indicate significant differences according to a one-way ANOVA (Tukey's test, $p < 0.05$).

TABLE 1 Correlation matrix showing the interrelationship between stem growth parameters and nutrient content

Variables	Stem height	Stem diameter	Amino acids content	Soluble sugars content	Starch content
Stem height		0.69	−0.78	−0.29	0.03
Stem diameter	$p < 0.0001$		−0.69	−0.51	−0.45
Amino acids content	$p < 0.0001$	$p < 0.0001$		0.49	0.13
Soluble sugars content	$p = 0.2033$	$p = 0.0058$	$p = 0.0071$		0.49
Starch content	$p = 0.8356$	$p = 0.0155$	$p = 0.8158$	$p = 0.0071$	

Note: Spearman correlations with associated adjusted *p*-values calculated with the Holm's method ($n = 40$ observations).

(Table 1). Interestingly, a negative correlation was shown between the inflorescence stem diameter/height and the total amino acids content as well as between the stem diameter and the soluble sugars and starch contents (Table 1). Additionally, a positive correlation between inflorescence stem height and diameter as well as a positive correlation between soluble sugars and starch contents were calculated (Table 1). These results suggest that the SWEET-dependent stem radial growth phenotype is associated with sugar and amino acid contents in this organ.

3.3 | Plant biomass production and seed yield are impaired in sweet mutant lines

Up to now, the effects of down or up-regulation of *SWEET11*, *SWEET12*, *SWEET16*, and/or *SWEET17* have been observed at an organ-specific level in rosette, stem, root, or seeds (Aubry et al., 2022; Chardon et al., 2013; Chen et al., 2012, 2015; Guo et al., 2014; Klemens et al., 2013; Le Hir et al., 2015; Valifard et al., 2021). Here, we wanted a more comprehensive view of the consequences of mutation in these genes on the aboveground organs at the end of plant development. For that purpose, the biomass produced by rosette leaves, stem (including the main, lateral, secondary stems, and the siliques envelopes), and seeds were assessed along with the analysis of C and N contents in each organ (Figure 3). Consistently to a previous report (Chen et al., 2012), rosette DW was significantly lower in the *swt11 swt12* double mutant (−45%) compared to the wild type (Figure 3A). The same decrease in rosette biomass is observed for the *swt-q* mutant, while no significant effect was measured in *swt16 swt17* (Figure 3A). Interestingly, a significant gain of biomass (about 40%) is measured only in the stem of the *swt16 swt17* double mutant (Figure 3A). Consistently with fewer siliques (Figure 1F), the seed yield was reduced in both *swt11 swt12* and *swt-q* mutant compared to wild-type plants (Figure 3A). We also estimated the C and N allocated to each organ in the 4 genotypes. In wild-type plants, N was allocated at 6%, 37%, and 57% to rosette, stem, and seeds, respectively (Figure 3B). In *swt11 swt12* and *swt-q* mutants, the N distribution was modified in all organs tested, with a significant decrease of N allocation in rosette and seeds, but a significant increase in the stem in both genotypes (Figure 3B). C was allocated at 3.5%, 33%, and 63.5% to rosette, stem, and seeds, respectively, in wild-type plants (Figure 3C). A significant decrease in C distribution was measured in the seeds of the *swt11 swt12* and *swt-q* mutants, while a significant increase of C was allocated to their stem (Figure 3C). Finally, the *swt16 swt17* double mutant displayed an intermediate phenotype for N and C allocation between WT and the other mutants (*swt11 swt12* and *swt-q*) but no statistical difference was measured compared to the wild type.

We also estimated the HI, which corresponds to the ratio of seeds DW to aboveground plant DW at harvest time. In our growth

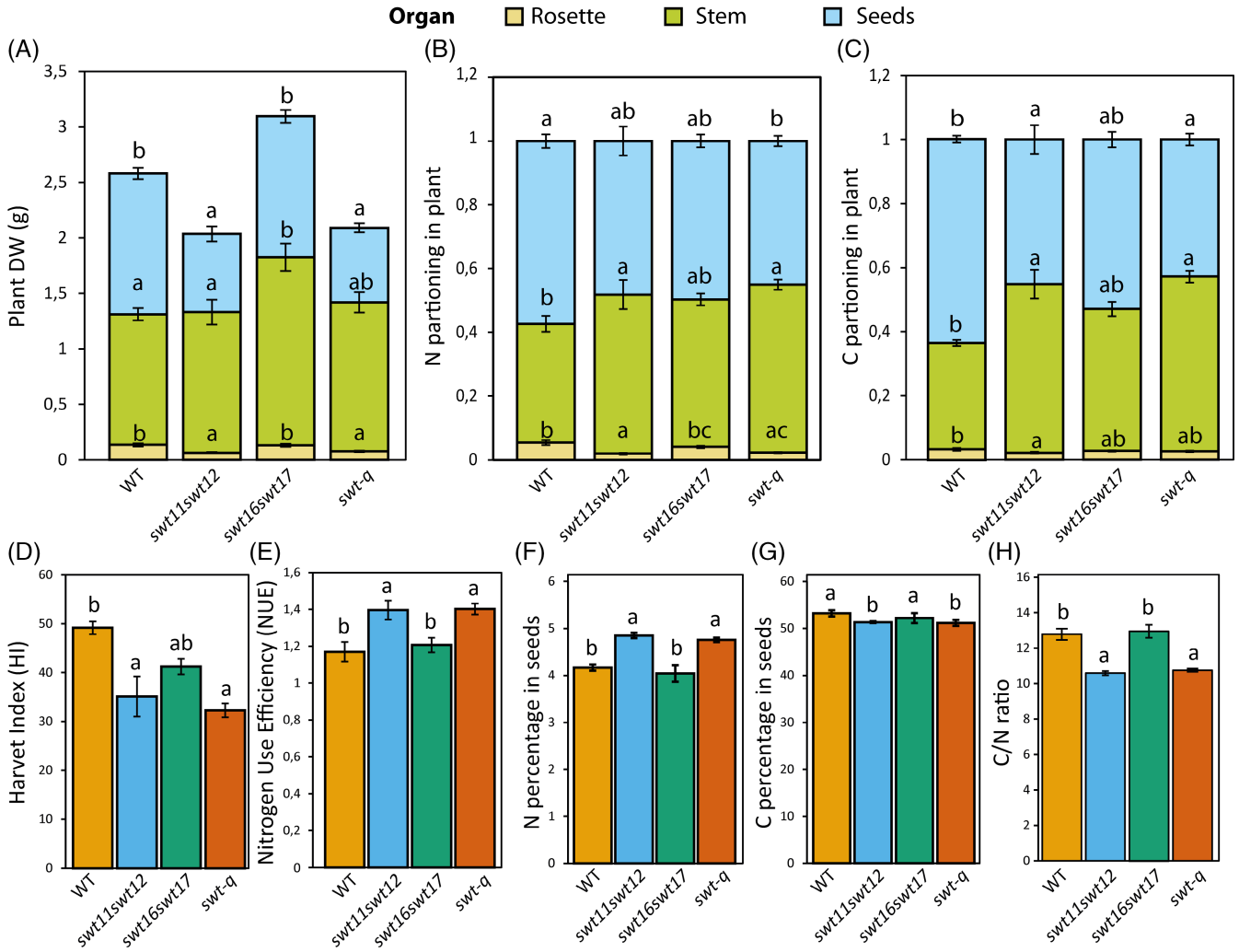

FIGURE 3 *SWEET* genes modulate plant biomass, yield, and NUE. (A–B) Barplots showing the dry weight (DW) (A) and the C/N ratio (B) in different plant parts (i.e., rosette leaves, total stem, and seeds) of wild type, *swt11 swt12*, *swt16 swt17*, and quadruple mutants. (C–D) Barplots showing the plant NUE (C) and the HI (D) for each genotype. Means ± SE are shown ($n \geq 5$ for each genotype). A one-way ANOVA combined with Tukey's comparison post-test has been made to compare the different genotypes. The different letters indicate significant differences.

conditions, HI represents about 50% of wild-type plants (Figure 3D). It was significantly lower (by about 70%) in the *swt11 swt12* and *swt-q* mutants, while no significant difference was observed for the *swt16 swt17* mutant compared to the wild type albeit with a similar tendency (Figure 3D). Since the *swt11 swt12* and *swt-q* mutants produce fewer seeds (lower HI) with a lower proportion of N in seeds (lower NHI), we determined the NUE as the ratio of NHI-to-HI to have information about the efficiency to store N in seeds irrespective of the plant capacity to produced seeds. Interestingly, we measured an improved NUE in the *swt11 swt12* and *swt-q* mutants compared to the wild type and the *swt16 swt17* mutant (Figure 3E). This suggests that *SWEET11* and *SWEET12* negatively impact the way the plant is efficiently using its nitrogen. Finally, we estimated the seed composition in the different genotypes and observed a significant decrease in the C percentage, while the N percentage significantly increased in the *swt11 swt12*, and quadruple mutants (Figure 3F,G). As a consequence, the C:N ratio of the seeds was significantly decreased in both genotypes (Figure 3H).

3.4 | Mutation in SWEET genes affects N remobilization efficiency

Despite an improved NUE in the *swt11 swt12* mutant, we observed a decreased C and N allocation to seeds in this genotype (Figure 3B,C,E). To understand in which organ the N flux might be blocked, we analyzed the ^{15}N partitioning to rosette, stem, and seeds in the different mutants (Figure 4). The use of ^{15}N labeling allows to estimate the plant's capacity to remobilize to the seeds the N compounds produced and stored in the rosette during the labeling period (Marmagne et al., 2020). In wild-type plants, 5% of ^{15}N remained in the rosette, 45% was stored in the stem, and 50% was remobilized to the seeds (Figure 4A–C). Our results show that consistently with a better NUE, less ^{15}N remains in the rosette of the *swt11 swt12* mutant (Figure 4A). A similar tendency, albeit not significant, was observed in *swt16 swt17*, and quadruple mutants compared to wild-type plants (Figure 4A). Interestingly, a

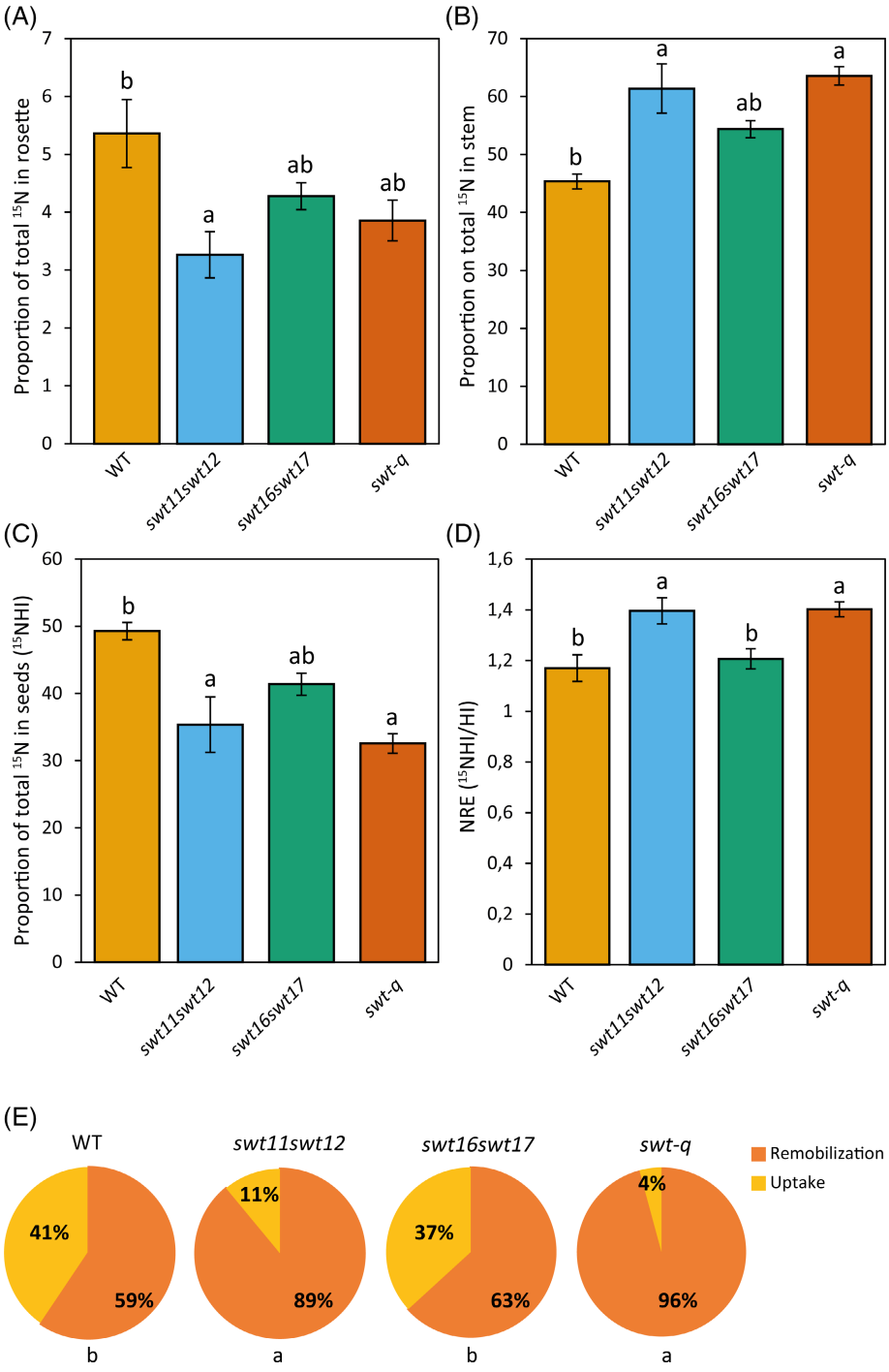

FIGURE 4 Nitrogen remobilization efficiency (NRE) is partly dependent on *SWEET* genes. (A–D) Barplots showing the proportion of total ^{15}N in the rosette (a), stem (B), seeds (C), and the NRE (D) in the wild type, *swt11 swt12*, *swt16*, *swt17* and quadruple mutants. (E) Pie charts showing the proportion of N originating from N remobilization or post-flowering N uptake in seeds of the wild type, *swt11 swt12*, *swt16 swt17*, and *swt-q* mutants. Means ± SE are shown ($n \geq 5$ for each genotype). A one-way ANOVA combined with Tukey's comparison post-test has been made to compare the different genotypes. The different letters indicate significant differences.

significant increased proportion of ^{15}N was measured in the stem of the *swt11 swt12* and *swt-q* mutants (Figure 4B), which led to a lower ^{15}N remobilization to the seeds (Figure 4C). Finally, the calculation of the NRE index allowed to determine if the ^{15}N partitioning to seeds is totally controlled by sink strength. In both the *swt11 swt12* and *swt-q* mutants, we observed a significant increase in the NRE index compared to the wild-type plants (Figure 4D). Altogether, these results show that disruption of *SWEET11* and *SWEET12* gene expression leads to better NUE and remobilization efficiency from the rosette. However, the N remobilized from the rosette accumulates in the stem at the expense of the seeds, most probably explaining the lower HI.

The nitrogen present in seeds comes from both N remobilization and post-flowering N uptake by the roots. Based on the results of the ^{15}N labeling, we could also deduce the proportion of both N origin in seeds (Marmagne et al., 2022). In wild-type plants, about 60% of N found in seeds comes from the remobilization process, while the remaining 40% is linked to the post-flowering N uptake (Figure 4E). Interestingly, in the *swt11 swt12* double mutant and the *swt-q* mutant, these proportions are severely impacted and the N part originated

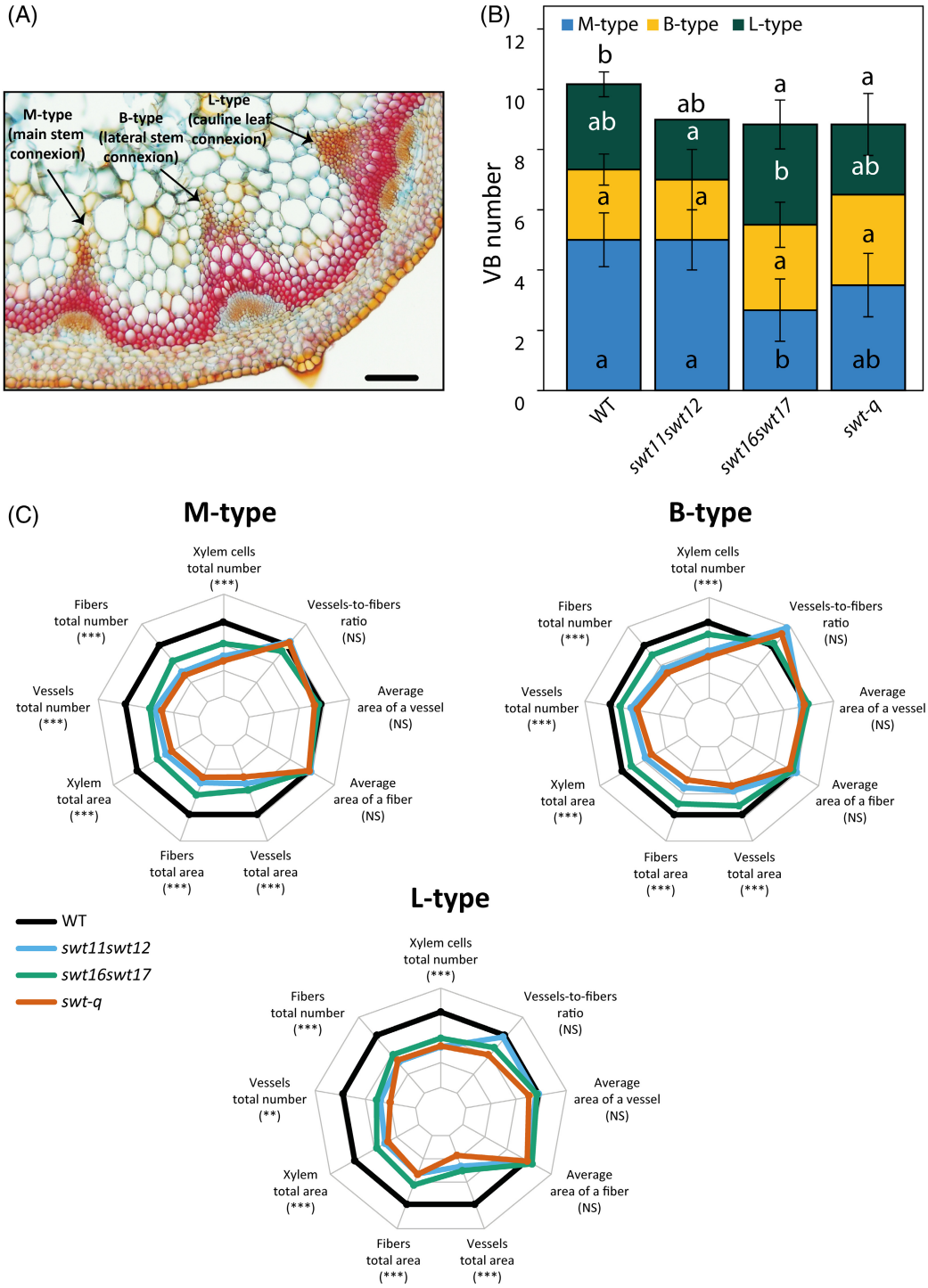

FIGURE 5 Mutation in *SWEET* genes affects vascular bundle (VB) development. (A) Photograph of the different VB types within an inflorescence stem cross-section showing the M-type, B-type, and L-type VBs. Scale bar = 100 µm. (B) Stacked histogram showing the number of each VB type in the different genotypes. Values are means ± SD (n = 5–6 plants). (C) Spider charts of anatomical traits describing the xylem tissue in M-type, B-type, and L-type VBs of the wild type, *swt11 swt12*, *swt16 swt17*, and *swt-q* mutants. The data are presented as the value of mutant lines over the value of WT plants set to 1 (black line). A one-way ANOVA combined with Tukey's comparison post-test has been performed on the raw data to compare the genotypes. The results of the ANOVA test are presented beside each VB type, and those of the Tukey's comparison post-test are presented in Figures S3–S5.

from post-flowering uptake is strongly reduced (Figure 4E). In the *swt16 swt17* double mutant seeds, the N coming from the post-flowering uptake is also slightly modified compared to wild-type seeds but the difference is not statistically different (Figure 4E). These results further strengthen the existence of an association of sugar transport with N uptake and remobilization to seeds.

3.5 | Quantitative analysis of the different VB types and impact of mutations in SWEET genes

Nitrate and amino acids are mostly transported in the xylem sap from leaves to seeds through the stem (Tegeder & Masclaux-Daubresse, 2018). Since we observed fewer xylem tissues in the stem of mutant lines together with improved nitrogen remobilization, we further explore the stem xylem defect by performing a quantitative analysis of the xylem in a vascular-bundle type manner (Figures 5 and S2–S5). Indeed, three different VB types can be observed in Arabidopsis stem: the M (main stem)-type VBs, which are the most common and are characterized by a triangular shape; the B (branch)-type VBs that are dividing VBs connected to a lateral inflorescence stem; and the L (leaf)-type VBs that are round-shaped VBs connected to the cauline leaf vasculature (Figure 5A). The M-type and B-type correspond to VBs involved in the root-to-shoot transport of water and N-derived nutrients to the seeds (Park et al., 2015). In wild-type plants, we observed around 10 VBs, among which 4–6 M-type VBs, 2–3 B-type VBs, and 2–3 L-type VBs (Figure 5B). When the expression of *SWEET11* and *SWEET12* is disrupted, no significant change in

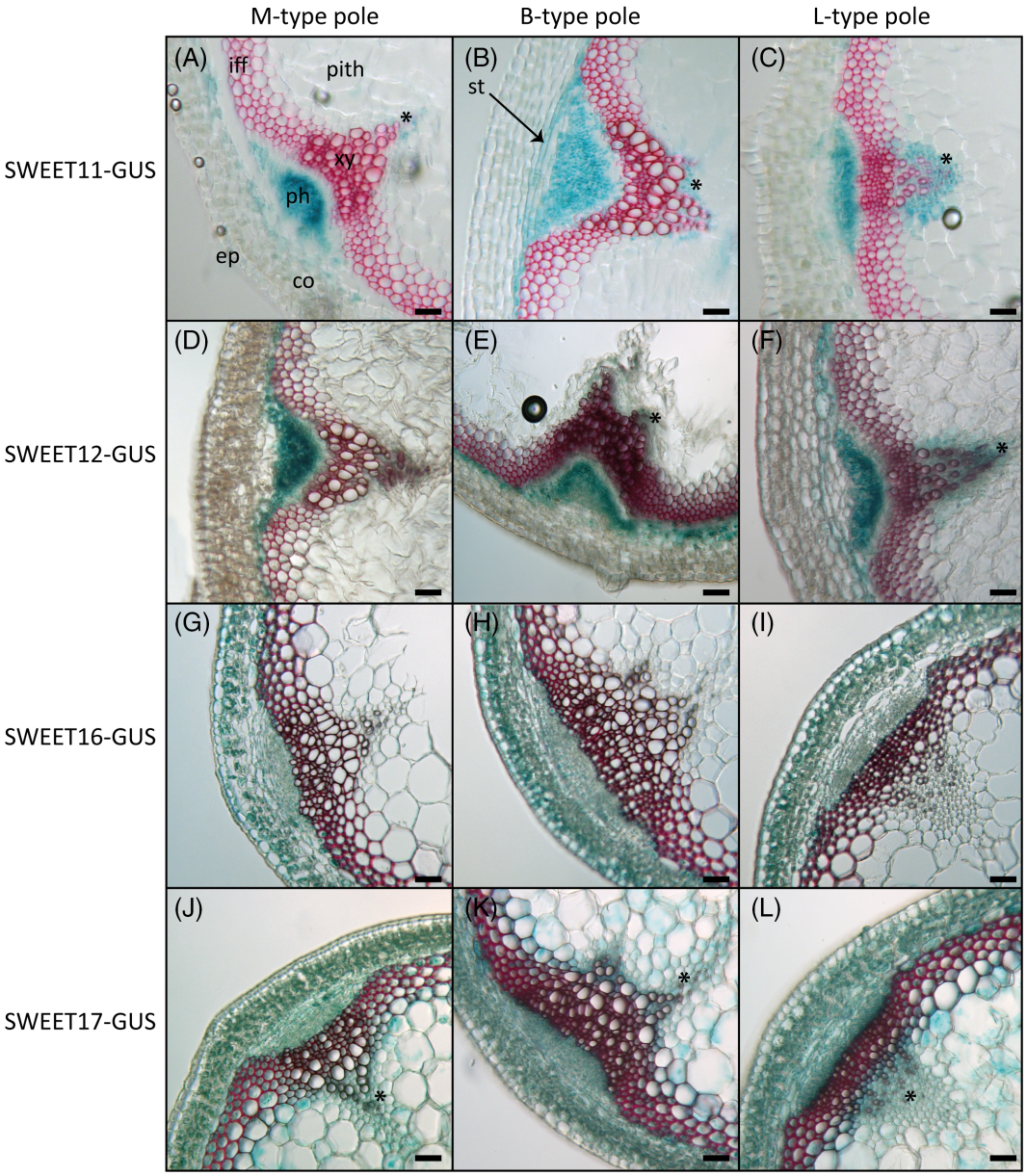

FIGURE 6 Expression patterns of SWEET11, 12, 16, and 17 in the different vascular bundle (VB) types and adjacent tissues. Histochemical analysis of GUS activity in lines expressing SWEET11-GUS (A)–(C), SWEET12-GUS (D)–(F), SWEET16-GUS (G)–(I), or SWEET17-GUS (J)–(L) fusion proteins driven by their native promoter in sections taken at the bottom of the inflorescence stem after 7 weeks of growth. Photographs show GUS expression in M-type VB (A, D, G, and J), in B-type VB (B, E, H, and K), or in L-type VB (C, F, I, and L). Asterisks point to cells showing blue GUS staining in xylem parenchyma cells. Lignin is colored pink after phloroglucinol staining. ep, epidermis; co, cortex; iff, interfascicular fibers; ph, phloem; st, starch sheath cells; xy, xylem.

the total number of VBs is observed (Figure 5B). However, when the expression of both genes coding for the tonoplastic SWEET16 and SWEET17 transporters is impaired, a significant decrease in the total number of VBs is observed compared to the wild-type plants (Figure 5B). Interestingly, in the *swt-q* mutant line, similarly to the *swt16 swt17* mutant, we also found fewer VBs compared to the wild-type plants (Figure 5B). While the same number of B-type VB is observed in the *swt16 swt17* double mutant compared to the wild type, significantly fewer M-type VBs and a tendency for more L-type VBs are observed in this mutant line (Figure 5B). In the *swt-q* mutant, a trend, albeit not significant, for less M-type and L-type VBs and more B-type VBs is observed (Figure 5B). Statistically, the *swt-q* mutant displays an intermediate phenotype between both double mutant lines, suggesting a possible additive role for plasmalemic and tonoplastic transporters in controlling the number of M-type VBs.

Several anatomical parameters, such as xylary fibers and xylem vessel numbers and sizes, were then measured to detail the morphological features of the different VB types. A PCA was applied to the dataset obtained on wild-type plants and allowed to observe a separation between the different VB types within the projection of the two first principal component planes that gather more than 83% of the total variation (Figure S2A). The first dimension clearly separates the B-type VB from the L-type VB, while the M-type VB presents an intermediate phenotype (Figure S2A). The number of xylem cells (xylary fibers and xylem vessels) and the area occupied by xylem vessels are the factors contributing the most to this separation (Figure S2B). The data show that B-type VBs are characterized by more and bigger xylary fibers than M-type VBs (Figure S2B). L-type VBs display fewer and smaller xylem vessels as well as a smaller fiber-to-vessel ratio than the M-type VBs (Figure S2B). In the mutant line, independently of the VB type, the *swt11 swt12*, and *swt-q* mutant lines displayed significantly fewer and smaller xylary fibers and xylem vessels (Figures 5C and S3–S5) than the wild type. Nonetheless, one exception is observed in the B-type VBs of the *swt11 swt12* double mutant for which no difference in the total number of vessels is observed compared to the wild type (Figure S4C). In addition, we observe that, compared to the wild type, *swt16 swt17* double mutant displayed significantly fewer and smaller xylem cells (including fibers and vessels) in M- and L-type VBs, but no significant effect was measured for B-type VBs (Figures 5C and S3–S5). These results suggest that a defect in the intercellular transport of sugars (via SWEET11 and SWEET12) predominantly impacts the xylem cell area and cell number rather than a defect in intracellular sugar transport (via SWEET16 and SWEET17).

3.6 | SWEET11, SWEET12, SWEET16, and SWEET17 have partially overlapping expression patterns in the vascular tissues of the stem independently of the VB type

Next, the translational GUS fusions lines previously described (Chen et al., 2012; Guo et al., 2014) were used to check the expression pattern of the different SWEET transporters in the different VB types (Figure 6). We observed that all four transporters are expressed both in phloem and xylem whatever the VB type (Figure 6). In the xylem tissue, SWEET11, SWEET16, and SWEET17 are expressed in the developing xylem cells (Figure 6B,H,K), while SWEET11, SWEET12, and SWEET17 are expressed in the xylem parenchyma cells located at the bottom of the VB in the protoxylem area (Figure 6A–F,J–L). This expression pattern is particularly visible in L-type VBs, which are mainly composed of parenchyma cells (Figure 6C,F,L). In addition, SWEET11 and SWEET12 are localized in the starch sheath cells, situated between the cortex and the phloem (Altamura et al., 2001) (Figure 6A–F). An expression of SWEET16 and SWEET17 is observed in the cortex cells and the interfascicular fibers (Figure 6G–L). Finally, SWEET17 is also expressed in some of the pith cells (Figure 6J–L).

4 | DISCUSSION

Modulation of inter or intracellular pool of sugars by modifying the expression of genes involved in sugar metabolism or transport modifies shoot and root growth, and plant yield in several species (e.g., Arabidopsis, Tomato, Tobacco, Poplar, and Pea) (Aubry et al., 2022; Dai et al., 1999; Le Hir et al., 2015; Lu et al., 2020; Mahboubi et al., 2013; Park et al., 2008; Stein et al., 2017; Valifard et al., 2021; Wingenter et al., 2010; Zhang et al., 2010). However, the effect of simultaneous disruption of sugar transport at both inter and intracellular levels has not been explored so far. In this study, we explored the effect on plant development and biomass production of the disruption of two genes coding for proteins involved in intercellular sugar transport (SWEET11, SWEET12) together with two genes coding for intracellular sugar transporters, (SWEET16 and SWEET17). *SWEET11* and *SWEET12* genes encode sugar transporters located at the plasma membrane of vascular parenchyma cells in leaves and stems (Cayla et al., 2019; Chen et al., 2012; Kim et al., 2021b; Le Hir et al., 2015). They were also shown to be expressed in seeds and roots (Chen et al., 2015; Desrut et al., 2020). On the other hand, *SWEET16* and *SWEET17* encode tonoplast-localized sugar transporters expressed in the vascular system of leaves, stems, and roots (Aubry et al., 2022; Chardon et al., 2013; Guo et al., 2014; Klemens et al., 2013; Valifard et al., 2021). Comparing the expression pattern of the four SWEET transporters in the inflorescence stem, we observed that they have partially overlapping expression patterns in the phloem, developing xylem cells, and xylem parenchyma cells. In addition, SWEET11 and SWEET12 are expressed in endodermis-like cells, which transiently store starch (also called starch sheath cells) (Altamura et al., 2001), and SWEET16 and SWEET17 in the cortex cells. Interestingly, the phenotype of the quadruple mutant is similar to that of the *swt11 swt12* double mutant for most of the traits related to plant biomass production and plant yield. On the other hand, the phenotype of the *swt16 sw17* double mutant was similar to that of the wild type or intermediate between the *swt11s wt12* and *swt-q* mutants. These results suggest that intercellular-facilitated transport of sugars, mediated by SWEET11 and SWEET12 expressed conjointly in the starch sheath cells, the phloem, and the xylem parenchyma, constitutes one limiting factor for plant biomass production

and plant yield. Moreover, the maintenance of the sugar homeostasis within the cell, regulated by SWEET16 and SWEET17, constitutes an important parameter for the regulation of the xylem and interfascicular fibers development, consistently with their expression in these cell types (Aubry et al., 2022).

In the stem, we show a perturbation of the C partitioning (including an accumulation of soluble sugars and starch) along with an expression of both SWEET11 and SWEET12 in the stem phloem tissue. These suggest that both transporters play a role in loading the phloem in the stem as previously shown in leaves (Chen et al., 2012). Moreover, our results show that, in stems, they are also likely involved in the starch remobilization from the starch sheath cells to the phloem parenchyma cells. These results are in line with stems being a major contributor to lifetime carbon gain during plant development (Earley et al., 2009). Especially, it has been shown that before the first siliques development, the main inflorescence stem stores carbon, such as starch, mainly in the endodermis-like cell layer above the phloem cells. Later in their development, stems are re-exporting nutrients to sustain silique development and seed maturation (Altamura et al., 2001; Durand et al., 2018; Ohmae et al., 2013; Sugita et al., 2016). However, to which extent perturbations of the C allocation in stems impact the C percentage in seeds is unclear. Part of the answer is provided by the C and N percentages in stems and seeds obtained by Chardon et al. (2014) on an Arabidopsis RIL population. Interestingly, while seed N% is positively correlated with stem N%, there is no significant correlation between seed C% and stem C%. These results suggest that C remobilization from the stem is much less important for seed filling than the N remobilization. Nonetheless, our results support that the lower C% in seeds measured in the *swt11 swt12* mutant could partially result from the overall defective sugar loading in this mutant. This will lead to lower delivery of carbon to the seeds because part of the C is not properly loaded or remobilized in the phloem sap from the stem and accumulated as starch in this organ. Interestingly, the defect in stem phloem loading could not only affect the sugar fluxes but could also explain why amino acids are accumulated in stems when the expression of *SWEET* genes is impaired. In particular, disruption of *SWEET11* and *SWEET12* dramatically reduced seed yield without altering the stem biomass production in the double and quadruple mutants. Because the sink strength is the key driver of N post-flowering uptake and N remobilization (Marmagne et al., 2022), we assumed that the reduction of seed yield leads to reduce N remobilization to seed. In addition, the ^{15}N partitioning in rosette is not increased in the mutants compared to WT, indicating that N mobilization from rosette to developing organs is not affected by these mutations. This suggests also that the amino acids loading in phloem from rosette are not impaired. Consequently, because the mobilization from the rosette is not affected and the allocation of ^{15}N to the seeds is reduced, the ^{15}N mobilization to the stem seems to be promoted, which may result in the amino acids accumulation measured in the stem. Thus, we propose that xylem defects in the stem constitute a bottleneck for the amino acid transfer to seeds. Our results support, therefore, that mutations in *SWEET11* and *SWEET12* globally impact either storage or phloem loading in the stem, including that of amino acids, thus limiting the N remobilization to the seeds. In addition, both *SWEET11* and *SWEET12* together with *SWEET15* have also been shown to be expressed in the different seed tissues (i.e., micropylar, endosperm, and seed coat) across its development (Chen et al., 2015). Consistently *swt11 swt12* and *swt11 swt12 swt15* mutant seeds display a decrease in their total fatty acid content (Chen et al., 2015). Therefore, the lower C% and C partitioning in the double mutant seeds could also be the consequence of the defect in sugar transport within the different tissues of the seed. On the other hand, the decreased N partitioning in seeds could result from a reduced transfer of amino acid from the stem to the seeds, affecting the quantity of amino acids delivered to the seeds. In the future, seed-specific complementation of the mutant phenotype could help to distinguish between the contribution of the stem or seed in seed carbon allocation defect.

In agriculture, one of the dilemmas to solve in the near future consists in improving the plant NUE to reduce production costs and environmental risks linked to N leakage in the environment. While manipulating the expression of amino acid transporters has been shown to efficiently improve NUE (Yang et al., 2020), the effect of deregulation of sugar transporters on NUE is scarce (Klemens et al., 2013; Schofield et al., 2009). This is surprising since C availability is known to be strongly associated with NUE (Fernie et al., 2020). In this study, we show that mutation in the expression of both *SWEET11* and *SWEET12* impact the N allocation at the whole plant level. Indeed, we measured (1) an increase of amino acids content in the stem, (2) an increase of N partitioning to the stem concomitantly with a decrease in seeds and rosette leaves, and (3) an increase of ^{15}N proportion in the stem and decrease in seeds. Ultimately, *swt11 swt12* double mutant displays an improved NUE and NRE despite a lower HI. Finally, *swt11 swt12* seeds display a lower C:N ratio, which points to a non-proportional enhancement of nitrogen supply (higher N%). In seeds of several species, such as sunflower, rapeseed, soybean and Arabidopsis, both C and N percentages are strongly correlated (Marmagne et al., 2020). Up to now, three hypotheses have been proposed to explain this phenomenon: (1) the dilution effect of the protein concentration by the enhanced oil concentration and vice versa; (2) the competition effect between C and N metabolisms for energy; and (3) the N availability effect, which suggests that the local N quantity and quality may affect the C and N metabolisms in siliques (Marmagne et al., 2020). In addition, we could also propose that the retention of C and N in *swt11 swt12* stem could also be responsible for this lower C:N ratio in seeds. In this context, a feedback mechanism consisting of a better NRE from the rosette leaves is used to compensate for the partial retention of N in the stem. Moreover, our results point out that the *swt11 swt12* double mutant also displays a defect in the post-flowering N uptake by the roots. Interestingly, in Arabidopsis seedlings, Chen et al. (2016) identified that the regulation of the expression of *SWEET11* and *SWEET12* by the shoot-to-root mobile transcription factor ELONGATED HYPOTOCOL5 (HY5) is required to modulate the expression of the nitrate transporter *NRT1.2*

in roots. Our results support this model and further suggest that SWEET16 and SWEET17 could also be considered since the *swt-q* mutant displays a tendency toward a further decrease in post-flowering N uptake, albeit not significant. Consistently, *swt17* single mutant showed defects in root growth and architecture (Valifard et al., 2021) that could also account for N uptake impairment since both traits are strongly linked (Kiba & Krapp, 2016). Altogether our results suggest that a proper sugar phloem loading mediated by SWEET11 and SWEET12 negatively impacts the way the plant uses and remobilizes its nitrogen to the seeds. However, to better apprehend the C and N fluxes in the different *swt* mutant lines, ^{13}C and ^{15}N labeling studies together with phloem and xylem sap composition measurements could be of interest.

To be transported long-distance, nutrients largely rely on the plant vascular system. Especially, the inflorescence stem constitutes the obligatory way for nutrients to be distributed from rosette leaves to seeds (van Bel, 2021). Consistently with our previous works on *swt11 swt12* and *swt16 swt17* double mutant lines (Aubry et al. 2022; Le Hir et al., 2015), we further show that the disruption of the expression of the four *SWEET* genes affects the vascular system expansion and tissue distribution. Especially the stem diameter decrease is likely due to the impaired development of cells undergoing important secondary cell wall formation (i.e., xylem and interfascicular fibers). As described by Park et al. (2015), three different types of VB with distinct functional features regarding water and mineral transport can be found in the Arabidopsis stem. In this study, we show that the VB types also display distinct anatomical features, consisting of different proportions of xylary fibers, xylem vessels, and xylem parenchyma cells. These observations suggest the existence of genetic control of their differentiation, which will most probably involve transcription factors responsible for the xylem cell type differentiation together with hormone regulation (Schuetz et al., 2012). Nonetheless, since sugars have also been shown to affect xylem development (Aloni, 1987), we hypothesize that changes in sugar availability, mediated by SWEET transporters, could be at play in the VB type differentiation. In line with this hypothesis, a lower number of VBs, mainly due to fewer M-type VBs, was found only in *swt16 swt17* mutant, along with a modified cellular morphology in the VBs involved in the connexion with the cauline leaves (L-type VB) and those responsible for long-distance transport of water and nutrients (M-type VB) (Park et al., 2015). Overall, these results suggest a possible reduced capacity for water and nutrient transport as well as reduced exchanges of these compounds between the stem and the cauline leaves. Nonetheless, since the plant yield is not affected in this mutant, it is likely that genetic compensation occurs to sustain normal seeds' quantity and quality. Therefore, the intracellular sugar fluxes mediated by SWEET16 and SWEET17 specifically affect the stem xylem development without impacting the plant yield in normal growth conditions. It could be of interest to test if the same holds true when plants are grown in limiting conditions such as osmotic stress for which xylem transport is important (Shafi et al., 2015; Shinohara et al., 2019). On the other hand, the defect in the sugar export/remobilization capacity in the stem likely account for the global stem growth and development phenotype observed in the *swt11 swt12* double mutant. Then, the resulting increased sugar storage in stems and leaves disturbs the plant's capacity to deal with N and, *in fine*, the plant yield.

Interestingly, a significant negative correlation was found between stem diameter and nutrient contents (i.e., soluble sugars, starch, and amino acids). Considering that stem diameter and nutrient contents could account for xylem development and C/N allocation, respectively, our results support a link between both traits. A role for sugars in vasculature development has been proposed for a long time, even if the identification of molecular actors involved starts only to emerge (for review Dinant & Le Hir, 2022). On the other hand, a similar role for amino acids has not been explored so far. Nonetheless, in tree stems, nitrogen addition, increased carbon allocation, or to a lesser extent, phosphorus addition, promote the enlargement of the vascular system (Plavcová et al., 2013; Cai et al., 2017; Hacke et al., 2017; Hartmann et al., 2020). On the opposite, in sunflower roots, a high root N has been associated with lower vessel number and size (Bowsher et al., 2016). Thus, this organ-dependent relationship between vascular development and C/N allocation highlights the complex interaction between both traits. A higher complexity level must also be added since nutrients act both as energy-provider compounds and signal molecules (Fichtner et al., 2021). Therefore, future studies exploring the link between nutrient allocation and vascular system development must consider a multiscale approach from tissue to the whole plant level.

5 | CONCLUSION

Our work proposes that SWEET11 and SWEET12 sugar transporters expressed in the stem's vascular system modulate both sugar and amino acid loading into the phloem sap, thus leading to an accumulation of sugars and amino acids in the stem. As a consequence, the nutrient transport between the stem and seeds is impaired, causing a decrease in plant growth, yield, and seed quality.

AUTHORS CONTRIBUTIONS

Beate Hoffmann: Investigation; methodology. **Emilie Aubry:** Investigation; methodology. **Anne Marmagne:** Investigation; methodology. **Sylvie Dinant:** Visualization; writing – review and editing. **Fabien Chardon:** Investigation; visualization; writing – review and editing. **Rozenn Le Hir:** Conceptualization; investigation; visualization; writing – original draft; writing – review and editing.

ACKNOWLEDGMENT

We thank Catherine Bellini for the critical reading of the manuscript.

FUNDING INFORMATION

This work has benefited from the support of IJPB's Plant Observatory technological platforms and from a French state grant (Saclay Plant

Sciences, reference ANR-17-EUR-0007, EUR SPS-GSR) managed by the French National Research Agency under the Investments for the Future program (reference ANR-11-IDEX-0003-02) through PhD funding to Emilie Aubry.

CONFLICT OF INTEREST

The authors declare that the research was conducted in the absence of any commercial or financial relationships that could be construed as a potential conflict of interest.

DATA AVAILABILITY STATEMENT

The data supporting the findings of this study are available from the corresponding author, Rozenn Le Hir, upon request.

ORCID

Anne Marmagne https://orcid.org/0000-0003-3466-9477
Sylvie Dinant https://orcid.org/0000-0001-6150-995X
Fabien Chardon https://orcid.org/0000-0001-7909-3884
Rozenn Le Hir https://orcid.org/0000-0001-6076-5863

REFERENCES

Aloni, R. (1987) Differentiation of vascular tissues. *Annual Review of Plant Physiology*, 38, 179–204.

Altamura, M.M., Possenti, M., Matteucci, A., Baima, S., Ruberti, I. & Morelli, G. (2001) Development of the vascular system in the inflorescence stem of Arabidopsis. *The New Phytologist*, 151, 381–389.

Aubry, E., Dinant, S., Vilaine, F., Bellini, C. & Le Hir, R. (2019) Lateral transport of organic and inorganic solutes. *Plants*, 8, 1–25.

Aubry, E., Hoffmann, B., Vilaine, F., Gilard, F., Klemens, P.A.W., Guérard, F. et al. (2022) A vacuolar hexose transport is required for xylem development in the inflorescence stem. *Plant Physiology*, 188, 1229–1247.

Baslam, M., Mitsui, T., Sueyoshi, K. & Ohyama, T. (2021) Recent advances in carbon and nitrogen metabolism in C3 plants. *International Journal of Molecular Sciences*, 22, 1–39.

van Bel, A.J.E. (2021) The plant axis as the command Centre for (re)distribution of sucrose and amino acids. *Journal of Plant Physiology*, 265, 153488.

Bowsher, A.W., Mason, C.M., Goolsby, E.W. & Donovan, L.A. (2016) Fine root tradeoffs between nitrogen concentration and xylem vessel traits preclude unified whole-plant resource strategies in Helianthus. *Ecology and Evolution*, 6, 1016–1031.

Braun, D.M., Wang, L. & Ruan, Y.L. (2014) Understanding and manipulating sucrose phloem loading, unloading, metabolism, and signalling to enhance crop yield and food security. *Journal of Experimental Botany*, 65, 1713–1735.

Cai, Q., Ji, C., Yan, Z., Jiang, X. & Fang, J. (2017) Anatomical responses of leaf and stem of *Arabidopsis thaliana* to nitrogen and phosphorus addition. *Journal of Plant Research*, 130, 1035–1045.

Cayla, T., Le Hir, R. & Dinant, S. (2019) Live-cell imaging of fluorescently tagged phloem proteins with confocal microscopy. *Methods in Molecular Biology*, 2014, 95–108.

Chardon, F., Bedu, M., Calenge, F., Klemens, P.A.W., Spinner, L., Clement, G. et al. (2013) Leaf fructose content is controlled by the vacuolar transporter SWEET17 in *Arabidopsis*. *Current Biology*, 23, 697–702.

Chardon, F., Jasinski, S., Durandet, M., Lécureuil, A., Soulay, F., Bedu, M. et al. (2014) QTL meta-analysis in Arabidopsis reveals an interaction between leaf senescence and resource allocation to seeds. *Journal of Experimental Botany*, 65, 3949–3962.

Chen, L.-Q., Lin, I.W., Qu, X.-Q., Sosso, D., McFarlane, H.E., Londoño, A. et al. (2015) A cascade of sequentially expressed sucrose transporters in the seed coat and endosperm provides nutrition for the Arabidopsis embryo. *Plant Cell*, 27, 607–619.

Chen, L.-Q., Qu, X.-Q., Hou, B.-H., Sosso, D., Osorio, S., Fernie, A.R. et al. (2012) Sucrose efflux mediated by SWEET proteins as a key step for phloem transport. *Science*, 335, 207–211.

Chen, X., Yao, Q., Gao, X., Jiang, C., Harberd, N.P. & Fu, X. (2016) Shoot-to-root mobile transcription factor HY5 coordinates plant carbon and nitrogen acquisition. *Current Biology*, 26, 640–646.

Dai, N., Schaffer, A., Petreikov, M., Shahak, Y., Giller, Y., Ratner, K. et al. (1999) Overexpression of Arabidopsis hexokinase in tomato plants inhibits growth, reduces photosynthesis, and induces rapid senescence. *Plant Cell*, 11, 1253–1266.

Desrut, A., Moumen, B., Thibault, F., Le Hir, R., Coutos-Thévenot, P. & Vriet, C. (2020) Beneficial rhizobacteria Pseudomonas simia WCS417 induces major transcriptional changes in plant sugar transport. *Journal of Experimental Botany*, 71, 7301–7315.

Dinant, S. & Le Hir, R. (2022) Delving deeper into the link between sugar transport, sugar signaling and vascular system development. *Physiol Plant*, 174(2), e13684.

Durand, M., Mainson, D., Porcheron, B., Maurousset, L., Lemoine, R. & Pourtau, N. (2018) Carbon source–sink relationship in *Arabidopsis thaliana*: the role of sucrose transporters. *Planta*, 247, 587–611.

Earley, E.J., Ingland, B., Winkler, J. & Tonsor, S.J. (2009) Inflorescences contribute more than rosettes to lifetime carbon gain in *Arabidopsis thaliana* (Brassicaceae). *American Journal of Botany*, 96, 786–792.

Fernie, A.R., Bachem, C.W.B., Helariutta, Y., Neuhaus, H.E., Prat, S., Ruan, Y. L. et al. (2020) Synchronization of developmental, molecular and metabolic aspects of source–sink interactions. *Nature Plants*, 6, 55–66.

Fichtner, F., Dissanayake, I.M., Lacombe, B. & Barbier, F. (2021) Sugar and nitrate sensing: a multi-billion-year story. *Trends in Plant Science*, 26, 352–374.

Gebauer, P., Korn, M., Engelsdorf, T., Sonnewald, U., Koch, C. & Voll, L.M. (2017) Sugar accumulation in leaves of Arabidopsis sweet11/sweet12 double mutants enhances priming of the salicylic acid-mediated defense response. *Frontiers in Plant Science*, 8, 1–13.

Grant, J.E., Ninan, A., Cripps-Guazzone, N., Shaw, M., Song, J., Petřík, I. et al. (2021) Concurrent overexpression of amino acid permease AAP1 (3a) and SUT1 sucrose transporter in pea resulted in increased seed number and changed cytokinin and protein levels. *Functional Plant Biology*, 48, 889–904.

Guo, W.-J., Nagy, R., Chen, H.-Y., Pfrunder, S., Yu, Y.-C., Santelia, D. et al. (2014) SWEET17, a facilitative transporter, mediates fructose transport across the tonoplast of Arabidopsis roots and leaves. *Plant Physiology*, 164, 777–789.

Hacke, U.G., Spicer, R., Schreiber, S.G. & Plavcová, L. (2017) An ecophysiological and developmental perspective on variation in vessel diameter. *Plant, Cell & Environment*, 40, 831–845.

Hartmann, H., Bahn, M., Carbone, M. & Richardson, A.D. (2020) Plant carbon allocation in a changing world—challenges and progress: introduction to a virtual issue on carbon allocation: introduction to a virtual issue on carbon allocation. *The New Phytologist*, 227, 981–988.

Le Hir, R., Spinner, L., Klemens, P.A.W., Chakraborti, D., De Marco, F., Vilaine, F. et al. (2015) Disruption of the sugar transporters AtSWEET11 and AtSWEET12 affects vascular development and freezing tolerance in Arabidopsis. *Molecular Plant*, 8, 1687–1690.

Hodges, M. (2002) Enzyme redundancy and the importance of 2-oxoglutarate in plant ammonium assimilation. *Journal of Experimental Botany*, 53, 905–916.

Huppe, H.C. & Turpin, D.H. (1994) Integration of carbon and nitrogen metabolism in plant and algal cells. *Annual Review of Plant Physiology and Plant Molecular Biology*, 45, 577–607.

Jasinski, S., Fabrissin, I., Masson, A., Marmagne, A., Lécureuil, A., Bill, L. et al. (2021) Accelerated cell death 6 acts on natural leaf senescence and nitrogen fluxes in Arabidopsis. *Frontiers in Plant Science*, 11, 1–15.

Kiba, T. & Krapp, A. (2016) Plant nitrogen acquisition under low availability: regulation of uptake and root architecture. *Plant & Cell Physiology*, 57, 707–714.

Kim, J.-Y., Loo, E.P.-I., Pang, T.Y., Lercher, M., Frommer, W.B. & Wudick, M.M. (2021a) Cellular export of sugars and amino acids: role in feeding other cells and organisms. *Plant Physiology*, 187, 1893–1914. Available from: https://doi.org/10.1093/plphys/kiab228

Kim, J.-Y., Symeonidi, E., Pang, T.Y., Denyer, T., Weidauer, D., Bezrutczyk, M. et al. (2021b) Distinct identities of leaf phloem cells revealed by single cell transcriptomics. *Plant Cell*, 33, 511–530.

Klemens, P.A.W., Patzke, K., Deitmer, J., Spinner, L., Le Hir, R., Bellini, C. et al. (2013) Overexpression of the vacuolar sugar carrier *AtSWEET16* modifies germination, growth, and stress tolerance in Arabidopsis. *Plant Physiology*, 163, 1338–1352.

Ladwig, F., Stahl, M., Ludewig, U., Hirner, A.A., Hammes, U.Z., Stadler, R. et al. (2012) Siliques are Red1 from Arabidopsis acts as a bidirectional amino acid transporter that is crucial for the amino acid homeostasis of siliques. *Plant Physiology*, 158, 1643–1655.

Le, S., Josse, J. & Husson, F. (2008) FactoMineR: an R package for multivariate analysis. *Journal of Statistical Software*, 25, 1–18.

Lu, M.Z., Snyder, R., Grant, J. & Tegeder, M. (2020) Manipulation of sucrose phloem and embryo loading affects pea leaf metabolism, carbon and nitrogen partitioning to sinks as well as seed storage pools. *The Plant Journal*, 101, 217–236.

Mahboubi, A., Ratke, C., Gorzsás, A., Kumar, M., Mellerowicz, E.J. & Niittylä, T. (2013) Aspen sucrose transporter3 allocates carbon into wood fibers. *Plant Physiology*, 163, 1729–1740.

Marmagne, A., Jansinski, S., Fagard, M., Bill, L., Guerche, P., Masclaux-Daubresse, C. et al. (2020) Post-flowering biotic and abiotic stresses impact nitrogen use efficiency and seed filling in *Arabidopsis thaliana*. *Journal of Experimental Botany*, 71, 4578–4590.

Marmagne, A., Masclaux-Daubresse, C. & Chardon, F. (2022) Modulation of plant nitrogen remobilization and post-flowering nitrogen uptake under environmental stresses. *Journal of Plant Physiology*, 277, 153781.

Meyer, R.C., Steinfath, M., Lisec, J., Becher, M., Witucka-Wall, H., Torjek, O. et al. (2007) The metabolic signature related to high plant growth rate in *Arabidopsis thaliana*. *Proceedings of the National Academy of Sciences*, 104, 4759–4764.

Müller, B., Fastner, A., Karmann, J., Mansch, V., Hoffmann, T., Schwab, W. et al. (2015) Amino acid export in developing Arabidopsis seeds depends on UmamiT facilitators. *Current Biology*, 25, 3126–3131.

Ohmae, Y., Hirose, A., Sugita, R., Tanoi, K. & Nakanishi, T.M. (2013) Carbon-14 labelled sucrose transportation in an *Arabidopsis thaliana* using an imaging plate and real time imaging system. *Journal of Radioanalytical and Nuclear Chemistry*, 296, 413–416.

Park, J., Kim, H.K., Ryu, J., Ahn, S., Lee, S.J. & Hwang, I. (2015) Functional water flow pathways and hydraulic regulation in the xylem network of Arabidopsis. *Plant & Cell Physiology*, 56, 520–531.

Park, J.Y., Canam, T., Kang, K.Y., Ellis, D.D. & Mansfield, S.D. (2008) Overexpression of an Arabidopsis family a sucrose phosphate synthase (SPS) gene alters plant growth and fibre development. *Transgenic Research*, 17, 181–192.

Paul-Victor, C. & Rowe, N. (2011) Effect of mechanical perturbation on the biomechanics, primary growth and secondary tissue development of inflorescence stems of *Arabidopsis thaliana*. *Annals of Botany*, 107, 209–218.

Perchlik, M. & Tegeder, M. (2018) Leaf amino acid supply affects photosynthetic and plant nitrogen use efficiency under nitrogen stress. *Plant Physiology*, 178, 174–188.

Plavcová, L., Hacke, U.G., Almeida-Rodriguez, A.M., Li, E. & Douglas, C.J. (2013) Gene expression patterns underlying changes in xylem structure and function in response to increased nitrogen availability in hybrid poplar. *Plant, Cell and Environment*, 36, 186–199.

Pouteau, S. & Albertini, C. (2009) The significance of bolting and floral transitions as indicators of reproductive phase change in Arabidopsis. *Journal of Experimental Botany*, 60, 3367–3377.

Pradhan Mitra, P. & Loqué, D. (2014) Histochemical staining of *Arabidopsis thaliana* secondary cell wall elements. *Journal of Visualized Experiments*, 87, 51381.

Rosen, H. (1957) A modified ninhydrin colorimetric analysis for amino acids. *Archives of Biochemistry and Biophysics*, 67, 10–15.

Schneider, C.A., Rasband, W.S. & Eliceiri, K.W. (2012) NIH Image to ImageJ: 25 years of image analysis. *Nature Methods*, 9, 671–675.

Schofield, R.A., Bi, Y.M., Kant, S. & Rothstein, S.J. (2009) Over-expression of STP13, a hexose transporter, improves plant growth and nitrogen use in *Arabidopsis thaliana* seedlings. *Plant, Cell and Environment*, 32, 271–285.

Schuetz, M., Smith, R. & Ellis, B. (2012) Xylem tissue specification, patterning, and differentiation mechanisms. *Journal of Experimental Botany*, 64, 11–31.

Sellami, S., Le Hir, R., Thorpe, M.R., Vilaine, F., Wolff, N., Brini, F. et al. (2019) Salinity effects on sugar homeostasis and vascular anatomy in the stem of the *Arabidopsis thaliana* inflorescence. *International Journal of Molecular Sciences*, 20, 3167.

Shafi, A., Chauhan, R., Gill, T., Swarnkar, M.K., Sreenivasulu, Y., Kumar, S. et al. (2015) Expression of SOD and APX genes positively regulates secondary cell wall biosynthesis and promotes plant growth and yield in Arabidopsis under salt stress. *Plant Molecular Biology*, 87, 615–631.

Shinohara, S., Okamoto, T., Motose, H. & Takahashi, T. (2019) Salt hypersensitivity is associated with excessive xylem development in a thermospermine-deficient mutant of *Arabidopsis thaliana*. *The Plant Journal*, 100, 374–383.

Sorin, C., Bussell, J.D., Camus, I., Ljung, K., Kowalczyk, M., Geiss, G. et al. (2005) Auxin and light control of adventitious rooting in Arabidopsis require ARGONAUTE1. *Plant Cell Online*, 17, 1343–1359.

Stein, O., Avin-Wittenberg, T., Krahnert, I., Zemach, H., Bogol, V., Daron, O. et al. (2017) Arabidopsis fructokinases are important for seed oil accumulation and vascular development. *Frontiers in Plant Science*, 7, 1–16.

Sugita, R., Kobayashi, N.I., Hirose, A., Saito, T., Iwata, R., Tanoi, K. et al. (2016) Visualization of uptake of mineral elements and the dynamics of photosynthates in Arabidopsis by a newly developed real-time radioisotope imaging system (RRIS). *Plant & Cell Physiology*, 57, 743–753.

Sulpice, R., Pyl, E.T., Ishihara, H., Trenkamp, S., Steinfath, M., Witucka-Wall, H. et al. (2009) Starch as a major integrator in the regulation of plant growth. *Proceedings of the National Academy of Sciences of the USA*, 106, 10348–10353.

Tegeder, M. & Masclaux-Daubresse, C. (2018) Source and sink mechanisms of nitrogen transport and use. *The New Phytologist*, 217, 35–53.

The, S.V., Snyder, R. & Tegeder, M. (2021) Targeting nitrogen metabolism and transport processes to improve plant nitrogen use efficiency. *Front Plant Science*, 11, 628366.

Tolivia, D. & Tolivia, J. (1987) Fasga: a new polychromatic method for simultaneous and differential staining of plant tissues. *Journal of Microscopy*, 148, 113–117.

Valifard, M., Le Hir, R., Müller, J., Scheuring, D., Neuhaus, H.E. & Pommerrenig, B. (2021) Vacuolar fructose transporter SWEET17 is critical for root development and drought tolerance. *Plant Physiology*, 187, 2716–2730.

Wingenter, K., Schulz, A., Wormit, A., Wic, S., Trentmann, O., Hoermiller, I. I. et al. (2010) Increased activity of the vacuolar monosaccharide transporter TMT1 alters cellular sugar partitioning, sugar signaling, and seed yield in Arabidopsis. *Plant Physiology*, 154, 665–677.

Xue, X., Wang, J., Shukla, D., Cheung, L.S. & Chen, L.-Q. (2022) When SWEETs turn tweens: updates and perspectives. *Annual Review of Plant Biology*, 73, 1–25.

Yang, G., Wei, Q., Huang, H. & Xia, J. (2020) Amino acid transporters in plant cells: a brief review. *Plants*, 9, 1–17.

Zhang, L., Tan, Q., Lee, R., Trethewy, A., Lee, Y.H. & Tegeder, M. (2010) Altered xylem-phloem transfer of amino acids affects metabolism and leads to increased seed yield and oil content in Arabidopsis. *Plant Cell Online*, 22, 3603–3620.

SUPPORTING INFORMATION

Additional supporting information can be found online in the Supporting Information section at the end of this article.

How to cite this article: Hoffmann, B., Aubry, E., Marmagne, A., Dinant, S., Chardon, F. & Le Hir, R. (2022) Impairment of sugar transport in the vascular system acts on nitrogen remobilization and nitrogen use efficiency in Arabidopsis. *Physiologia Plantarum*, 174(6), e13830. Available from: https://doi.org/10.1111/ppl.13830